

# ON THE LINK BETWEEN MARTIAN TOTAL OZONE AND POTENTIAL VORTICITY

**J. A. Holmes**, *School of Physical Sciences, The Open University, Milton Keynes, MK7 6AA, UK, (james.holmes@open.ac.uk)*, **S. R. Lewis**<sup>1</sup>, **M. R. Patel**<sup>1,2</sup>, <sup>1</sup>*Department of Physical Sciences, The Open University, Milton Keynes, MK7 6AA, UK,* <sup>2</sup>*Space Science and Technology Department, STFC Rutherford Appleton Laboratory, Chilton, Didcot, Oxfordshire, OX11 0QX, UK.*

## Introduction:

Potential vorticity (hereafter PV) is a dynamical tracer which is a product of the absolute vorticity and static stability of the atmosphere. PV can be redistributed but neither created or destroyed on an isentropic surface in the absence of friction and diabatic processes [1].

The conservation principle explains why PV is used to study polar vortices on Earth. PV contains information on winds and temperature in a single scalar variable and the motion of air is generally parallel to contours of PV [2]. The invertibility of PV is also an important property, since given sufficient boundary conditions PV can be inverted to deduce the flow of the whole atmosphere. Changes in the PV distribution thus 'induce' changes in the wind and temperature fields.

On Earth, studies have found a significant positive PV-ozone correlation in both global maps of total ozone from satellite observations [3] and local profiles of ozone at multiple observatories [4,5], particularly at mid to high latitudes in the winter hemisphere (Figure 1). While the relationship of ozone and PV on Mars has never before been investigated, a strong correlation between PV, a dynamical tracer, and ozone suggests several applications such as using ozone observations to study the dynamical behaviour of the polar vortices and using PV as a proxy for ozone in polar winter.

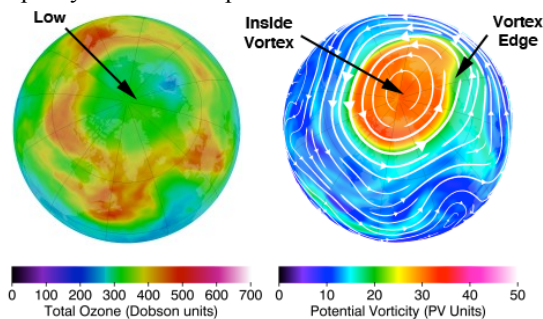


Figure 1 - Northern hemisphere total ozone (left) and PV (right) on the 460K surface for 22 February 2011. White lines on the PV image are streamlines, where the thickness of the streamlines and size of the arrows indicate the strength of the local flow. Image courtesy of NASA Ozone Watch.

Observations of ozone over several Mars years have been collected by the Mars Color Imager [6] on

the Mars Reconnaissance Orbiter, and therefore interannual variations or trends in the dynamical state of the polar vortices can be investigated. Current satellite observing techniques to retrieve ozone cannot however reach high poleward latitudes in polar night, where the largest amounts of ozone exist and ozone is effectively a quasi-passive tracer due to the lack of destruction mechanisms [7]. If a strong correlation is apparent between PV and ozone at poleward latitudes in polar night, the spatial distribution of PV, which can be constrained by reanalysis datasets [8,9], can be used as a proxy for ozone to extend the coverage of total ozone observational datasets. This technique has already been performed successfully on Earth [10,11].

## Atmospheric modelling:

To investigate the link between PV and ozone on Mars, the UK version of the LMD Mars GCM (hereafter MGCM) is used. The model has been developed in a collaboration of the Laboratoire de Météorologie Dynamique, the Open University, the University of Oxford and the Instituto de Astrofísica de Andalucía.

The MGCM uses physical parameterisations accounting for CO<sub>2</sub> condensation and sublimation, sub-grid scale dynamics, vertical diffusion and convection (amongst others) coupled to a spectral dynamical core and semi-Lagrangian advection scheme [12] to transport tracers. Using a spectral model, spatial derivatives are calculated exactly, and so the calculation of PV is more accurate than previous attempts using temperature observations and interpolation methods [13].

Ozone, along with 14 other tracers, is adjusted chemically by the LMD photochemical model [7] which provides an extensive analysis of photochemical and chemical interactions in the martian atmosphere.

## Results:

The zonally-averaged daily-mean distribution of total ozone and PV for MY 29 can be compared in Figure 2. PV is seen to decrease tracing a path from either pole to the equator over the whole year, as expected due to the decrease in planetary vorticity and static stability at lower latitudes. The largest

values of PV are seen in the polar winter of each hemisphere, with the northern hemisphere winter slightly increased (maximum of  $9.24 \times 10^{-4} \text{ K kg}^{-1} \text{ m}^2 \text{ s}^{-1}$ ) when compared to the southern hemisphere winter (maximum of  $[-]8.79 \times 10^{-4} \text{ K kg}^{-1} \text{ m}^2 \text{ s}^{-1}$ ). For the majority of the respective winter season in each hemisphere, the distribution of PV is also seen to display an annular nature, as reported by [9]. Maximum PV anomalies are seen away from the pole at a latitude of between  $75\text{--}85^\circ$  in both southern and northern winter.

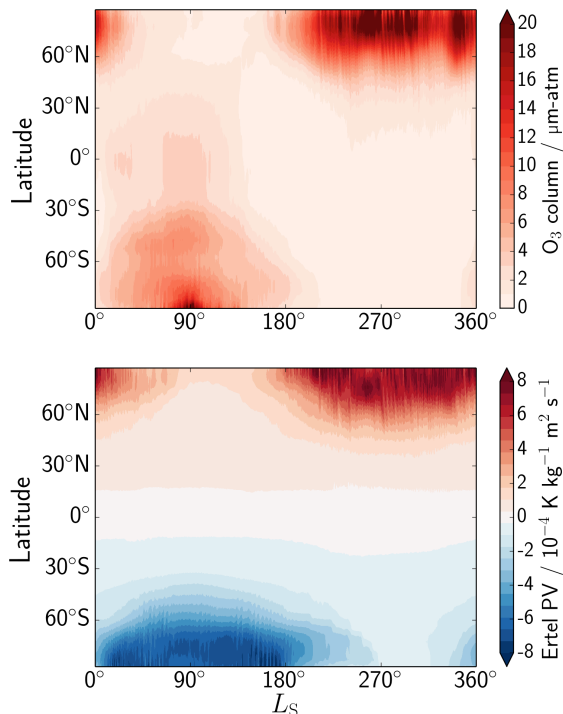


Figure 2 – Zonally-averaged daily-mean total ozone (top) and Ertel potential vorticity on the 260 K surface (bottom) for one whole Mars year.

The ozone cycle on Mars is thoroughly explored in [7] and briefly detailed here. Maximum total ozone values are found in polar winter due to the lack of sunlight preventing photolysis of ozone. The primary destructors of ozone, odd hydrogen species, are also largely absent with the cooler temperatures meaning much less water vapour (the primary source of odd hydrogen species) is present in the atmosphere. Increased values of total ozone are apparent in northern winter when compared to southern winter due to the weaker wave activity of the southern high latitudes [7].

At lower latitudes, there is increased total ozone in the first half of the martian year as a result of the vertical distribution of water vapour. The cold and dust-free atmosphere results in a low saturation altitude of water vapour around 10–15 km, allowing ozone to build above this hygropause [7]. The hygropause level increases in the second half of the martian year, resulting in less ozone at higher alti-

tudes and therefore decreased total ozone. Heterogeneous uptake of odd hydrogen species (included in the simulation) on water ice clouds [14] also contributes to the increased total ozone in the first half of the year due to the presence of the aphelion cloud belt.

The summer season in both hemispheres is dominated by minimal total ozone since photolysis of ozone rapidly decreases the column total during the day, with slightly increased values at nighttime. Total ozone is at a minimum in southern summer ( $L_S = 225\text{--}315^\circ$ ) at poleward southern latitudes since this region is in almost constant daylight and Mars is at perihelion meaning a shorter but more intense summer with maximal heating from the Sun.

*PV-total ozone correlation.* The day-to-day PV-total ozone correlation for northern and southern polar regions in Mars Year 29 are shown in Figure 3. For poleward northern latitudes, a very strong PV-total ozone correlation of  $r = 0.8$  or greater is found for 274 sols in the year.

In northern summer, the PV-total ozone correlation decreases as expected, and in some cases even goes negative. Over this time period ( $L_S = 75\text{--}150^\circ$ ), small amounts of total ozone and PV are found, but PV is still increased poleward primarily due to the planetary vorticity being largest at this location. Total ozone is more abundant away from the pole causing the negative correlation.

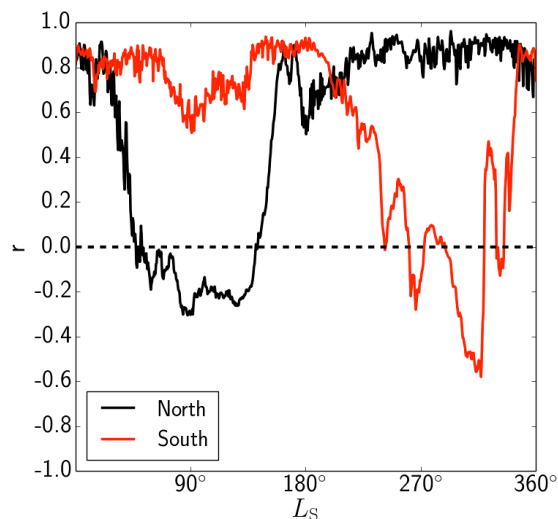


Figure 3 – PV-total ozone correlation for northern (black) and southern (red) latitudes for Mars year 29 covering latitudes  $35\text{--}90^\circ$  in both hemispheres. PV is sampled on the 260K surface. The dashed black line indicates zero correlation.

In the southern hemisphere, the variation in topography at latitudes further south than  $35^\circ\text{S}$  provides preferential sites for a localized increase of ozone. Ozone will reach high levels in the Hellas and Argyre basins due to the high surface pressure (hence large atmospheric column mass) at these lo-

cations providing an ideal setting for the accumulation of ozone near the ground [7]. This contributes to a slight weakening of the PV-total ozone correlation in the middle of southern polar winter.

*Northern polar winter.* A snapshot of the total ozone and PV spatial distribution in northern polar winter ( $L_S = 292^\circ$ ) is displayed in Figure 4. The PV-total ozone correlation for this case study is  $r = 0.826$ . The strong PV-total ozone correlation on a short daily time scale suggests that the variations in total ozone are largely due to dynamical influences, as to be expected for winter when chemical reactions are at a minimum.

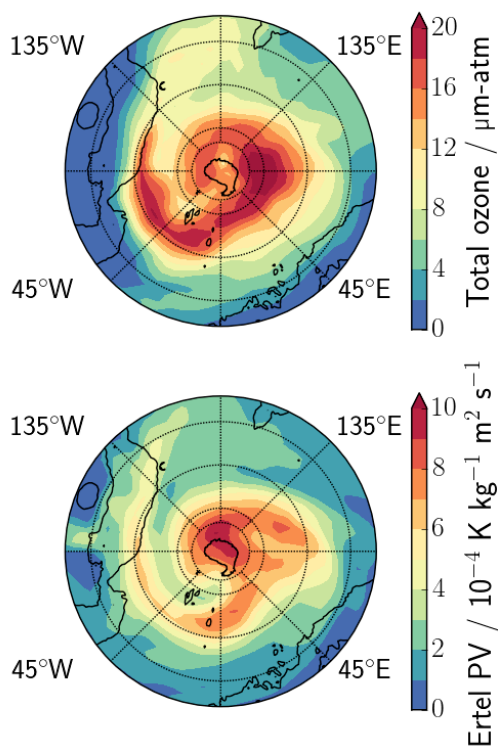


Figure 4 – Northern polar projection of total ozone (top) and PV (bottom) during northern polar winter at  $L_S = 292^\circ$ . Black contours indicate topography.

A filament of PV can be seen from 0-135°W in Figure 4, which corresponds well to a similar feature in the total ozone distribution, further strengthening the possibility of using PV as a proxy for total ozone (and vice versa). PV has been used on Earth to track the polar vortices and has recently been used equivalently for Mars [9]. The martian polar vortex also provides an excellent barrier for the mixing of chemical tracers, suggesting that total ozone in the winter season, when it is quasi-passive, can potentially be used to track the shape of the polar vortex.

Further results will be discussed at the conference, including the first ever calculation of the ozone/PV ratio on Mars.

## References:

- [1] Haynes P. H. and McIntyre M. E. (1987) *J. Atmos. Sci.*, 44, 828–841.
- [2] Holton J. R. and Hakim G. J. (2004) *Academic press*.
- [3] Vaughan G. and Price J. D. (1991) *Q. J. Roy. Meteor. Soc.*, 117, 1281–1298.
- [4] Beekmann M. et al. (1994) *J. Geophys. Res.*, 99, 12841–12851.
- [5] Rao T. N. et al. (2003) *J. Geophys. Res-Atmos.*, 108, 4703.
- [6] Clancy R. T. et al. (2016) *Icarus*, 266, 112–133.
- [7] Lefèvre F. et al. (2004) *J. Geophys. Res.*, 109, E07004.
- [8] Montabone L. et al. (2014) *Geoscience Data Journal*, 1, 129–139.
- [9] Mitchell D. M. et al. (2015) *Q. J. Roy. Meteor. Soc.*, 141, 550–562.
- [10] Randall C. E. et al (2002) *J. Geophys. Res-Atmos.*, 107, 8299.
- [11] Randall C. E. et al. (2005) *J. Atmos. Sci.*, 62, 748–764.
- [12] Newman C. E. et al. (2002) *J. Geophys. Res.*, 107, 5123.
- [13] McConnochie T. H. (2007) *Ph.D. thesis, Cornell University*.
- [14] Lefèvre F. et al. (2008) *Nature.*, 454, 971–975.